

Application of Water Balance and SWAT Model for Groundwater Recharge Estimation: Beressa Watershed, Central Ethiopian Plateau, Ethiopia.

Thalada. Suryanarayana¹ Amanuel Godie Gigar² Zeleke Simachew Anteneh³
Tiliksew Wasie Bihonegn⁴

¹Professor of Geology, College of Natural Sciences, Department of Geology, Wollo University, Dessie, Ethiopia.

²Lecture of Hydrogeology, College of Natural Sciences, Department of Geology, Wollo University, Dessie, Ethiopia.

³Lecture of Geology, College of Natural Sciences, Department of Geology, Wollo University, Dessie, Ethiopia.

⁴Lecture of Hydrogeology, College of Natural Sciences, Department of Geology, Wollo University, Dessie, Ethiopia.

Corresponding Author Name: Prof. Suryanarayana Thalada

ABSTRACT

Recharge is an important parameter in groundwater flow and transport models. Sustainable groundwater management also requires knowledge and quantification of groundwater recharge. Quantifying groundwater recharge is thus a prerequisite for efficient and sustainable groundwater resource management. As aquifers are depleted, recharge estimates have become more essential in determining appropriate levels of groundwater withdrawal. Water balance and SWAT models have been applied to estimate the annual groundwater recharge of Beressa watershed, which is part of the Blue Nile Basin in the central Ethiopian highlands. The results from the water balance method show that from annual precipitation of 947 mm, 641 mm re-evaporates to the atmosphere, 169 mm follows surface runoff and 136 mm percolates through the water table to the groundwater system. The three water balance components account for 67.66%, 17.91% and 14.44% of the annual precipitation, respectively. The result from the SWAT model shows annual evapotranspiration of 572 mm, surface runoff 228 mm, interflow 25 mm and annual groundwater recharge of 126 mm. This accounts for 60.42%, 24.12%, 2.69% and 13.35% of the annual precipitation, respectively. The amount of annual sustainable yield is also estimated to be 40% of the recharge, 17.93 MCM.

Keywords: Groundwater Resource Management, Water Balance, SWAT Models, Recharge, Watershed

Date of Submission: 15-12-2022

Date of Acceptance: 30-12-2022

I. Introduction

1.1 Background

Water is a precious natural resource, without which there would be no life on Earth and its occurrence is the main factor, which makes our Planet, The Earth, unique in the solar system. Similarly, it constitutes two-thirds of the weight of our body. Our everyday lives depend on the availability of cheap and clean water resources, which are also important for agricultural and industrial activity (Kevin Hiscock, 2005). Groundwater is water stored in the saturated zone with in rocks below the water table. Groundwater plays a major role in the livelihood of humankind by providing water for drinking, irrigation, and industrial purposes. Groundwater obtained from beneath the Earth's surface is often cheaper, more convenient and less vulnerable to pollution than surface water (Kevin Hiscock, 2005, Saied Eslamain, 2014). Water is the most common substance on the surface of the Earth, covering over 70 percent of the planet. However, about 96.54 percent of the total amount of water is in the oceans and is not directly usable. Similarly, glaciers and ice caps cap 1.74 percent of the total water. This makes Groundwater the most abundant (1.69 %) water resource for direct household and other human consumptions on the planet (Tim Davie, 2008).

According to (Freeze and Cherry, 1979), groundwater recharge is the entry into the saturated zone of water made available at the water-table surface. Recharge is an important parameter in groundwater flow and transport models. Sustainable groundwater management also requires knowledge and quantification of groundwater recharge. Quantifying groundwater recharge is thus a prerequisite for efficient and sustainable groundwater resource management. As aquifers are depleted, recharge

estimates have become more essential in determining appropriate levels of groundwater withdrawal (KetemaTilahun, 2009).The study shows the presence of an increasing large scale urban sprawling in the area. The city is also becoming center of huge industries, which require large supply of water resource and a number of water bottling factories. This, along with the increasing urbanization and population increase is expected to exert pressure on the quality and quantity of groundwater resources within the Beressa watershed. Hence, estimation of the annual amount of water being recharged for the aquifers in the watershed is an important and effective tool for wise utilization and management of the groundwater resource. This study assesses the annual groundwater recharge of the watershed using two techniques, Water Balance (WB) and SWAT model.

1.2 Location and Accessibility

Beressa watershed is found in central Ethiopia, within the North Shoa zone of Amhara administrative region around 130 Km North-East of Addis Ababa. Hydrologically, it is found within the Jema sub-basin of Blue Nile Basin along its Southeastern boundary with the Awash Basin, covering an area of 340 Km². administratively, it is found within three Woredas of North Shoa Zone: Angolela Tera, Debre Birhan Zuria and Debre Birhan Town administration (Figure 1). Astronomically, the watershed is found between longitude 39.46° E and 39.73° E and latitude 9.56° N and 9.75° N. The watershed is accessible through the main Addis Ababa-Dessie-Mekelle main asphalt road.

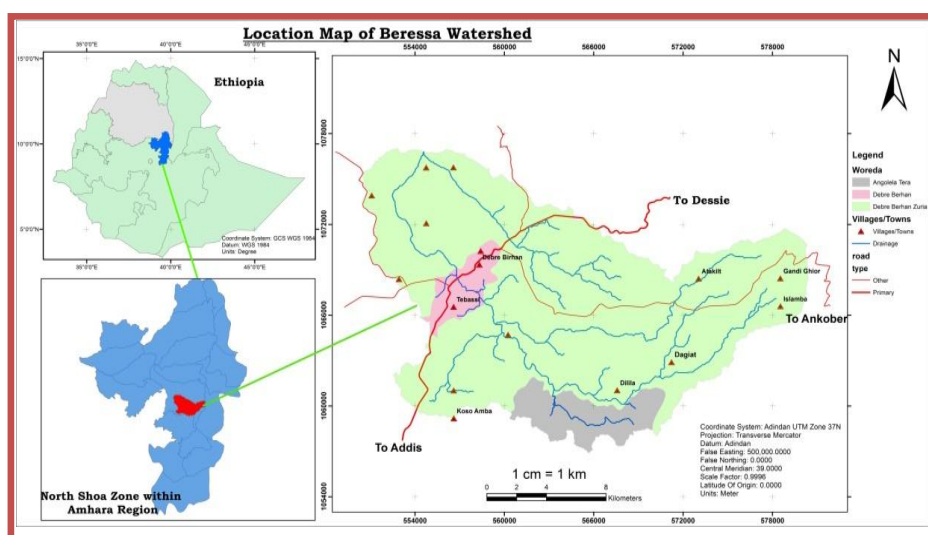


Figure 1: Location map of Beressa watershed

1.3 Objectives

The main objective of this study is to estimate annual groundwater recharge of the watershed using WB and SWAT mode

Specific objectives include:

- ✓ To characterize the area in terms of physiography, drainage, soil cover, Land Use Land Cover (LULC), geology and hydrogeology.
- ✓ To estimate average annual water balance components, Precipitation, Evapotranspiration, Runoff and Groundwater recharge using WB and SWAT model
- ✓ To compare groundwater recharge estimation using the two methods.
- ✓ To estimate the amount of sustainable yield in the watershed

1.4. Methodology and Materials

The methodology employed to accomplish the objectives set above is principally a desk study of different data for the given watershed. The watershed is delineated in Arc SWAT interface using 30 m resolution SRTM Digital Elevation Model (DEM) data downloaded from open topography website (<http://opentopo.sdsc.edu/datasets>). The drainage pattern of streams is also extracted similarly. The LULC data of the watershed is clipped from Sentinel-2 LULC map of Ethiopia for the year 2016. On the other hand, FAO digital soil map of Ethiopia is used to characterize the soil type of the watershed. The geology and hydrogeology of the area is characterized based on data obtained from the Geological Survey of Ethiopia (GSE). Daniel Meshesha, et al., 2010, has studied the geology of Debre Birhan area and produced the geological map of the Debre Birhan map sheet at a scale of 1: 250,000 based on field observations, petrographic studies, Landsat image analysis and literature studies. Whereas, Hydrogeological and Hydrochemical Maps of Debre Birhan map sheet was made by collaboration of Czech Geological Survey and Geological Survey of Ethiopia, 2018. To estimate the groundwater recharge based on WB method, daily precipitation data for ten years (2004-2013) is utilized from CFSR (Climate Forecast System Reanalysis) dataset. Monthly average Potential Evapotranspiration (PET) and Actual Evapotranspiration (AET) is calculated using Thornthwaite method. The average annual runoff for the watershed is calculated using Curve Number (CN) method. The annual groundwater recharge of the watershed is then calculated as the residual of the two water balance components from the annual precipitation.

II. Watershed Characteristics

2.1. Size and Shape

The size of a watershed is best explained in terms of its area (A) and Perimeter (P), whereas Gravelius coefficient or compactness index (K) can be used to express its shape. The area of Beressa watershed is 340.594 km² and its perimeter is 141 km calculated using Arc map. Gravelius coefficient or compactness index (K), devised by Gravelius, and expresses the ratio of the perimeter of the drainage basin to that of a circle of equal area.

$$k = \frac{141 \text{ km}}{\sqrt{2 \cdot 3.14 \cdot 340.594 \text{ km}^2}} = 2.155787$$

The compactness index shows that the watershed is not circular in shape, it is rather elongated. The visual shape of the watershed can be seen from the location map given above.

2.2. Physiography and Slope

The local physiography of the area has been characterized based on SRTM 30m DEM data. The topography shows three distinct classes: rugged mountainous region in the Eastern part of the watershed (along the recharge areas), extensive plateau region in the central and southern part of the watershed and localized, deep and rugged gorges in the northwestern region along the outlet of the watershed. The elevation of the watershed ranges from 2099m to 3646m a.s.l from the deep gorges to the mountainous terrains, respectively.

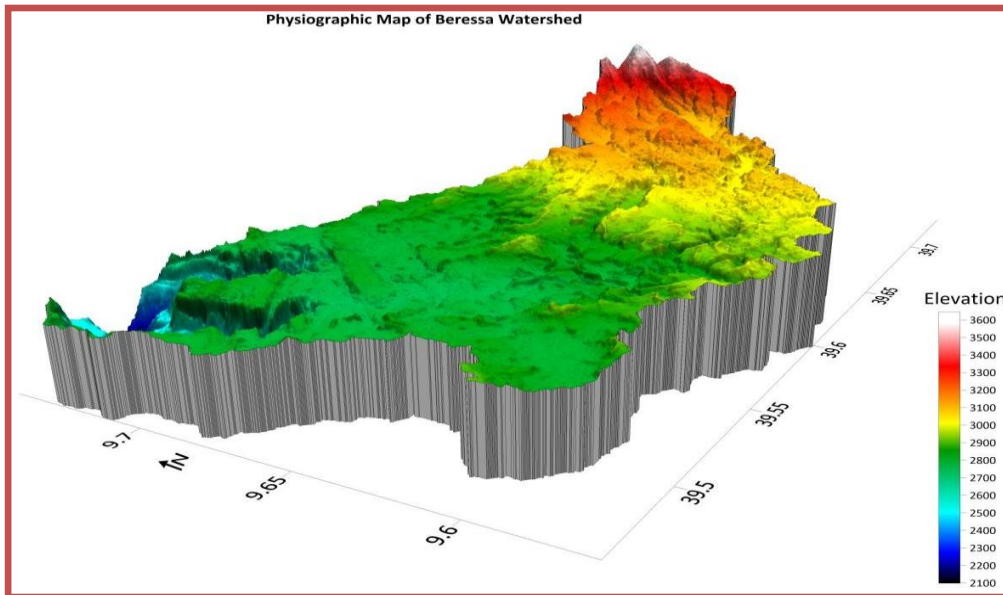


Figure 2: Physiographic map of Beressa watershed

Slope gradient of the study watershed is classified into five classes: 0-5, 5-11, 11-19, 19-31, 31-74 degrees, which represent from near horizontal to very steep slope areas. The highest slopes are found in the river gorges and mountains, where as the central plateau areas are relatively near horizontal.

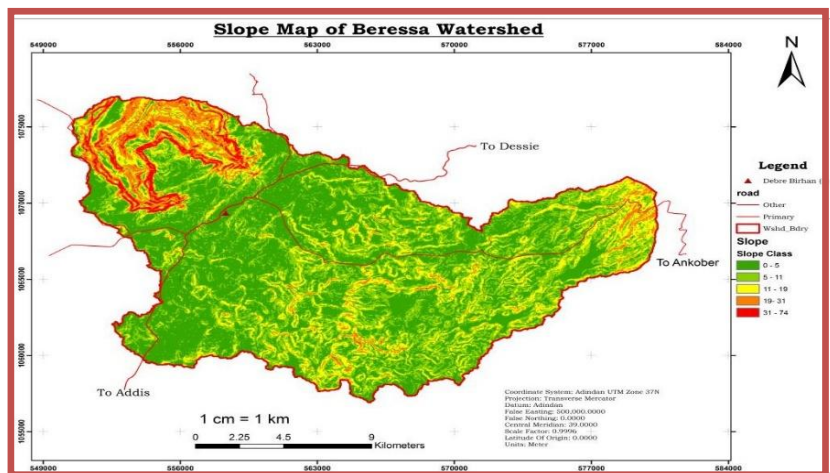


Figure 3: Slope map of Beressa watershed

2.3. Drainage Density and Drainage Pattern

Streams and rivers in the Beressa watershed start from the eastern part of the area and drain first to southwest and then to northwest towards the watershed outlet. The two major rivers in the watershed are Beressa and Dalecha rivers. Beressa River is perennial, whereas Dalecha River is intermittent and the two rivers bound DebreBirhan city from South-West and North- East direction, respectively. The drainage pattern of the river networks is not the same at different sectors of the watershed. It has semi-parallel drainage pattern on the eastern and southwestern side (downstream and upstream areas), while dendritic drainage pattern is observed in the central part.

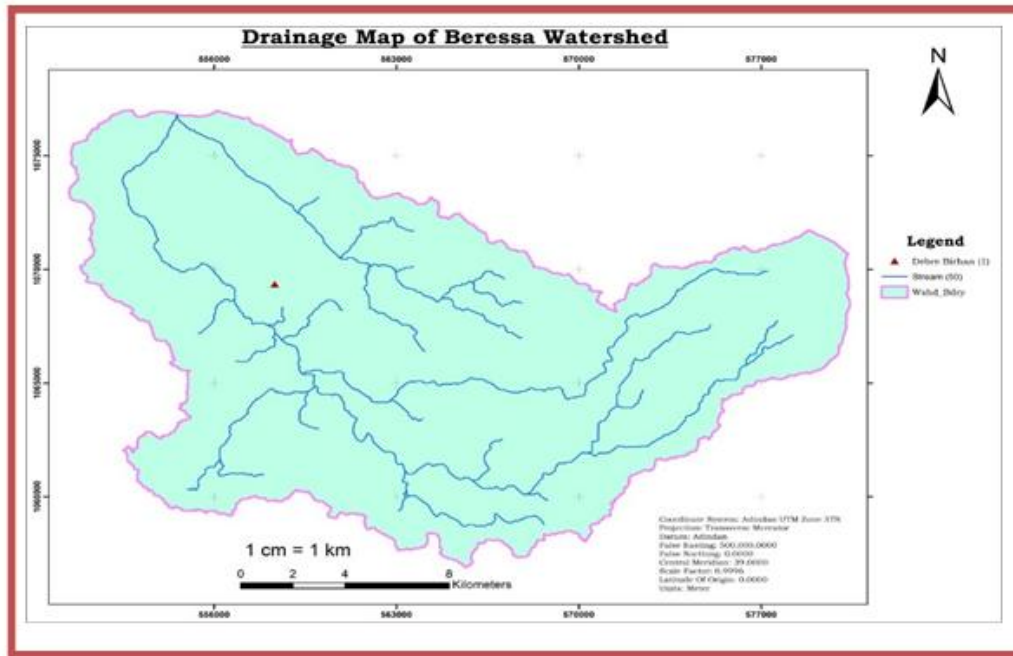


Figure 4: Drainage map of Beressa watershed

2.4. Climate

The climate of Ethiopia is mainly controlled by the seasonal migration of the Inter-tropical Convergence Zone (ITCZ) following the position of the sun relative to the earth and the associated atmospheric circulation. It is also highly influenced by the complex topography of the country. There are five traditional climate classes in the country: Wurch (representing very cold climate at elevations greater than 3000m a.s.l), Dega (representing temperate like climate in the highlands with altitude range of 2500-3000m asl), WoinaDega (warm climate representing areas with altitude ranges of 1500-2500m a.s.l), Kola (hot and arid type climate in an areas with elevation less than 1500m a.s.l) and Bereha (typical of areas with very hot and hyper-arid climate)(NMSA, 2001). According to this classification, Beressa watershed lies within three different climate regions: Wurch, Dega and WoinaDega. Most part of the area lies within Dega climate region, where as Wurch and WoinaDega climate types are constrained to the Upstream and Downstream areas of the watershed.

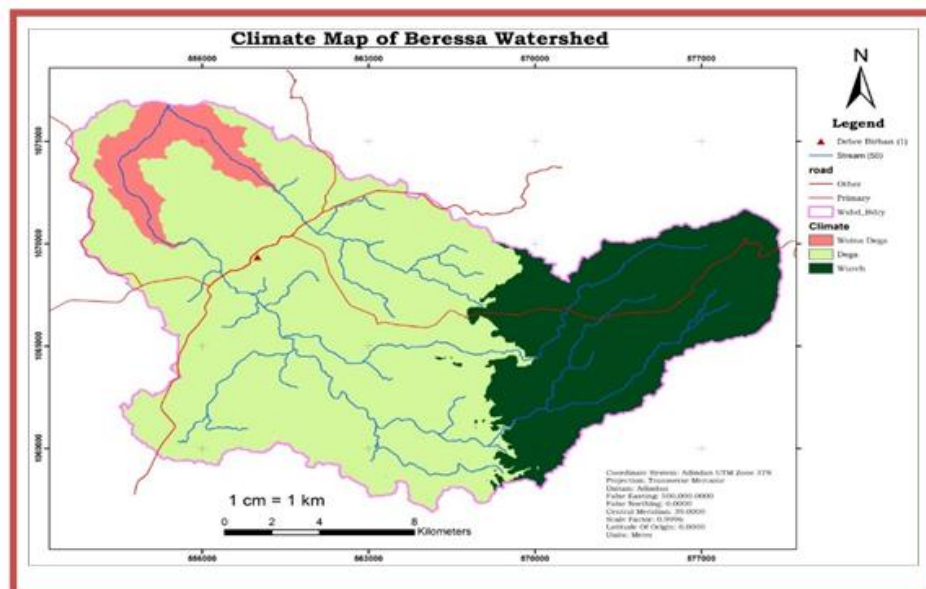


Figure5: Climate map of Beressawatershed

2.5. Land Use Land Cover (LULC)

The LULC of an area is one of the most important determinant factors for the water resource potential of an area. In groundwater recharge, it controls areas of rainfall percolation and runoff generating areas. The LULC data of the area was found from 20m resolution Sentinel- 2 LULC map of Ethiopia.

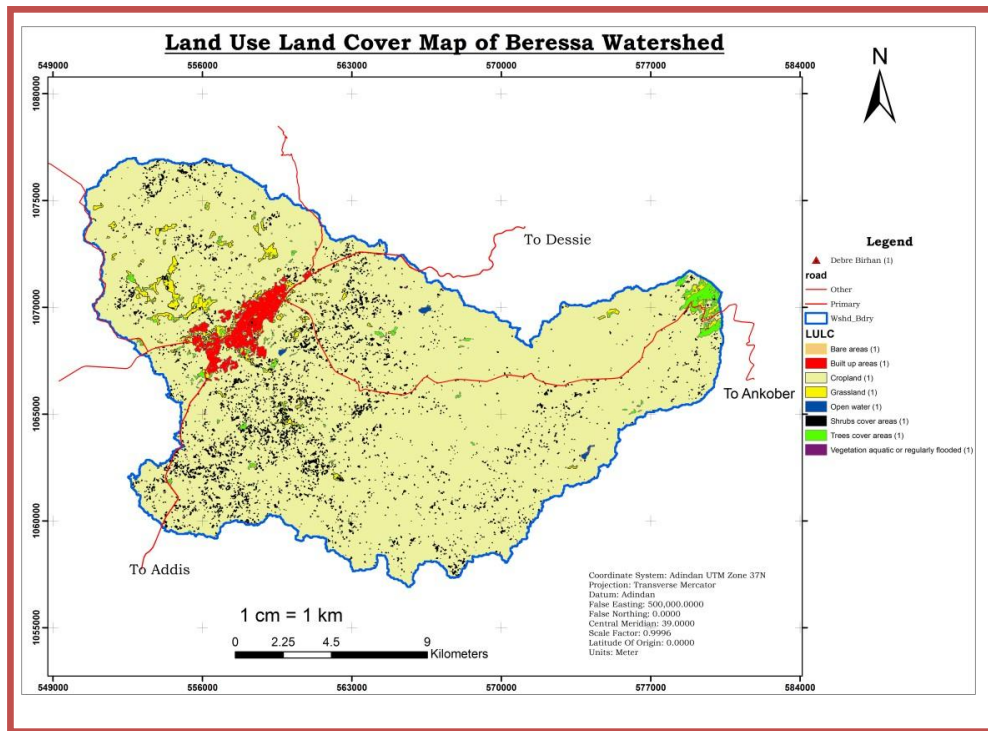


Figure6:LULCmapofBeressa watershed

2.6. Soil

The soil groups of Beressa watershed are classified according to the FAO soil group. As a result, three soil classes are distinctly mapped: VerticCambisols (CMv), EutricLeptosols (LPe) and Lithic Leptosols (LPq). Cambisols holds soils with incipient soil formation. Based on data from (BeleteBerhanu et al., 2013) the hydrologic group of the soils is classified as B and D.

Textureclass	Effective watercapacity(Cw)(mm)	Infiltration rate (f)(mm/hour)	Hydrologic soilgrouping
Sand	8.89	210.1	A
Loamy sand	7.874	61.2	A
Sandyloam	6.35	25.9	A
Loam	4.826	13.2	B
Silt loam	4.318	6.9	B
Sandyclay loam	3.556	4.3	C
Clayloam	3.556	2.3	D
Siltyclayloam	2.794	1.5	D
Sandyclay	2.286	1.3	D
Siltyclay	2.286	1.0	D
Clay	2.032	0.5	D

Table 1: Soil Infiltration rate and hydrological soil group based on textural class (adopted from BeleteBerhanu et al., 2013)

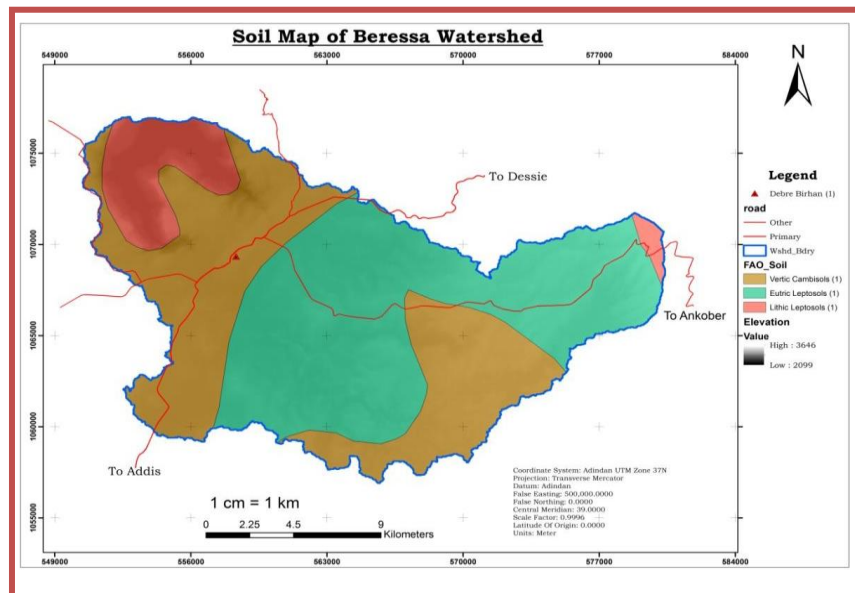


Figure 8: Soil map of Beressa Watershed

III. Geology And Hydrogeology Of Beressawatershed

3.1 Geology of Beressa Watershed

Beressa watershed is located within the central Ethiopian Plateau along the Northwestern margin of Main Ethiopia Rift System. According to Daniel Meshesha et al (2010), the study area consists of litho-stratigraphic units, Cenozoic volcanic rocks and Quaternary superficial deposits. Cenozoic volcanic rocks, which are found in the study area, are formed during the tertiary volcanism and these rocks include Tarmaber-Megezez basalt and Sela Dengay-Debre Birhan-Gorgo ignimbrite. On the other hand, a Quaternary superficial deposit common in the watershed is Eluvium deposit.

3.1.1 Lithostratigraphic units

The main governing factor for the hydraulic characteristics of ground water is the rock units, which found in the area. To characterize the hydraulic properties of the rocks in the area we have used local and regional previously worked data. Accordingly, the area is covered by three different lithologic units, which have different age and history. These rock units are represented as follow in age wise from oldest (Sela Dengay-Debre Birhan-Gorgo ignimbrite) to youngest (Eluvium) superficial deposits.

Sela Dengay-Debre Birhan-Gorgo Ignimbrite

According to Daniel Meshesha et al (2010), this unit has sharp contacts with the overlying (Tarmaber-Megezez,) and underlying (Kesem) basalts. It comprises ignimbrite, rhyolite, Tertiary sediment, tuffaceous sediment, aphanitic basalt, agglomerate and ash. The ignimbrite forms gentle to steep cliffs, elongated ridges and sporadically distributed isolated hills. It is medium to coarse grained, light/bluish/brownish gray-to-gray (fresh color) to dull/dark gray (weathering color), highly consolidated to welded tuff and bedded. It also shows columnar joint, vertical joints, and fractures.

Tarmaber-Megezez Basalt

According to Daniel Meshesha et al (2010), it has sharp contact with the underlying Sela Dengay-Debre Birhan-Gorgo ignimbrite. Tarmaber-Megezez basalt includes fine, medium to coarse-grained, dark gray (fresh color) to light/reddish/dark/yellowish brown (weathering color) and aphanitic to porphyritic basalts. It is characterized by different phases of basaltic flows separated by randomly exposed reddish palaeosols and reddish brown scoriaceous basalts (0.5-8m thick). It is dominantly represented by plagioclase phyric varieties (plagioclase phyric and olivine-plagioclase phyric basalts) together with minor olivine phyric, pyroxene phyric, plagioclase-pyroxene-olivine phyric and aphanitic basalts. It is medium to coarse grained and dark gray, containing plagioclase phenocrysts up to 5cm in length. Petrographic studies of the plagioclase phyric basalt show an average composition of groundmass 35%, plagioclase 30%, pyroxene (augite) 10%, olivine 12% and opaque minerals 10 percentage.

Eluvium Deposits

According to Daniel Meshesha et al (2010), the eluvium soil is mostly found on the plateau and escarpment of the map sheet, occupying flat lying and gentle topography cover small part of the study area. The gradual weathering of the basalt, ignimbrite and rhyolite forms it. There are rock fragments of basalt, ignimbrite and rhyolite within the eluvium soil. It is silt to clay sized, light/dark gray to reddish brown fertile soil. It is highly ploughed by the local people.

3.1.2 Geological Structures

As presented above the area is dominated by volcanic rock types so the hydraulic properties of the rocks are controlled by primary and secondary geological structures. Since the study area is found along the western margin of main Ethiopian rift valley secondary geological structures are common. Among the common secondary geological structures in the area include faults, joints and shear zones we may act as a conduit for water movement in the subsurface and they will increase the permeability of associated rock units.

Normal Faults

In the study area, two sets of normal faults are observed as shown in the geological map. These Normal faults are NE-SW (including boundary faults and several rift oriented step faults) and NW-SE trending transcurrent faults. In the rift margin, the NE-SW trending normal faults are characterized by a series of parallel step faults having different magnitudes. The NE-SW trending faults have similar orientation with the major main Ethiopian rift border fault, while the NW-SE trending faults are nearly perpendicular with the major regional border faults. Along with the major lithological rock units in the study area, these faults will have an effect on the storage and on the ground water; dynamics and this will affect the quality of aquifer.

Joints and Irregular Fractures

Fractures are discontinuities of rock units formed after the formation of the rock units due to brittle deformation.

The orientation and the degree fracturing control ground water dynamics. Differently oriented joint sets and irregular fracture (few mm to cm in width) are observed in the Beressa watershed. They are penetrative to non-penetrative joints, having significantly variable strike length. Mostly in the ignimbrite two sets of joints are encountered, these are horizontal (dipping 30° towards SE) and vertical (trending N-S and N10°E) set of joints. In addition irregularly oriented columnar joint sets (mostly hexagonal faces) are also observed in the ignimbrites and basalts (Jiri Sima, 2018).

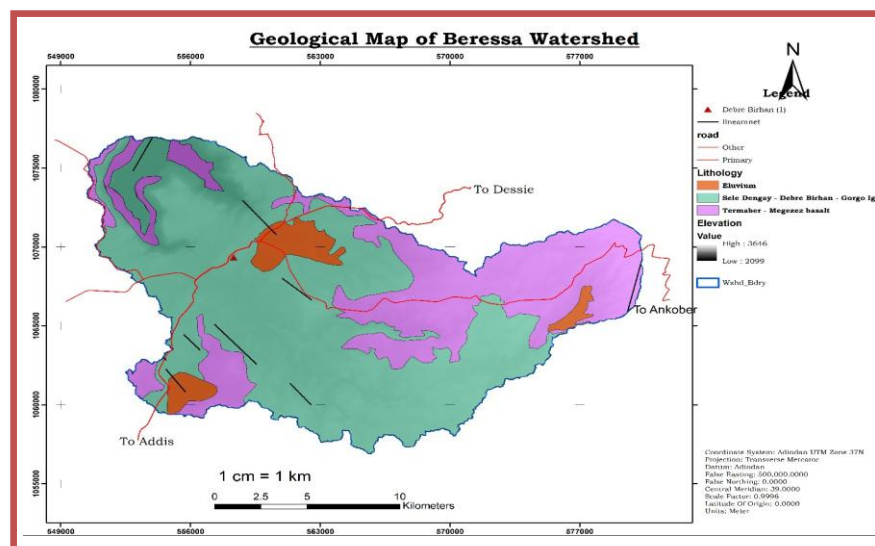


Figure 9: Geological map of Beressa watershed (adopted from Daniel Meshesha et al., 2013)

3.2 Hydrogeology of the area

From the hydrogeological point of view, a good aquifer must be sufficiently permeable and transmissive with interconnected pores and fissures and with enough storage to yield groundwater. The groundwater bearing potential is also related to faults, and weathered and fractured zones in the rock mass. According to the (Jiri Sima, 2018), geological units are a major factor that control the quantity and quality of groundwater occurrence in the area. Sedimentary rocks have great potential for groundwater due to their high primary porosity and permeability relative to other rocks. Reclassifying lithostratigraphic units into hydro stratigraphic units requires information on the hydraulic characteristics of rocks.

Hydraulic Characteristics of Tarmaber-Megezez Basalt

These basalts have an average yield of wells of 10 l/s and springs of 6 l/s, and are aquifers with very good secondary porosity and permeability (Jiri Sima, 2018). These basalts are tectonically affected by the NNE-SSW trending normal faults, which follow the rift propagation. These structures enhance the recharge conditions of the area and, in addition to the intensive development of fractures, weathered rock and joints in this unit create favorable conditions for their good permeability.

Hydraulic Characteristics of Sela Dengay-Debre Birhan-Gorgo Ignimbrite

Sela Dengay-Debre Birhan-Gorgo-Ignimbrite/Trachyte/Rhyolite/Tertiary sediments aquifers of the plateau with an average discharge of well = 10 l/s and spring = 1.3 l/s and the boreholes sunk in the fractured ignimbrite have transmissivity of between 0.05 and 226 m²/day and a mean transmissivity of 100.3 m²/day (Jiri Sima, 2018). It is highly consolidated to welded tuff and bedded with columnar joints, vertical joints, and fractures. These fissured and mixed aquifers of the plateau represent the most important hydrogeological unit of the area.

Hydraulic Characteristics of Eluvium Deposits

The eluvium is mostly found on the plateau and escarpment, occupying flat lying and gentle sloping topography. The gradual weathering of the basalt, ignimbrite and rhyolite forms a thick cover of Regolith. There are fragments of basalt, ignimbrite and Rhyolite within the eluvial soil. The regolith is from silt to clay in size, and light/dark gray to reddish brown in color. Dug Wells are used for the purposes of community water supply (Jiri Sima, 2018). Generally, the eluvium is the most important hydrogeological unit in the area especially for shallow groundwater sources.

IV. Ground Water Recharge Estimation

4.1 Water Balance Method

Groundwater recharge is the process by which water percolates down the soil and reaches the water table either by natural or artificial methods to replenish the aquifer with water from the land surface (Teklebirhan, A. et al, 2012). The estimation of groundwater recharge is regarded as a highly challenging parameter in hydrogeology. It is one of the most important components in hydrogeological characterization of aquifer systems and the major objectives in hydro-meteorological studies (Berehanu, B. et al, 2017). Ground water at a basin level can be estimated/quantified using various methods. This method is attractive, because it can be applied almost anywhere precipitation data are available. However, there is a drawback of the water balance method due to shortcomings inherent to the techniques used. Nonetheless, despite its shortcomings, the water-balance method is a powerful tool to understand the main features of recharge processes, if short time steps are used and the spatial variability of components is taken into account (Berehanu, B. et al, 2017).

4.2.1 Water Balance Components

The basic concept of water balance method within a given period is:

Input to the system - Outflow from the system = Change in storage of the system.

The inflow and outflow components used in groundwater estimation include the following:

a) Precipitation

Precipitation is the main input (inflow) component used in the calculation of ground water recharge. Isohyets is used to determine the Isohytal area and the average of the two consecutive Isohyets is used as the precipitation value for that area. Finally, each weighted precipitation is summed up to estimate the total average annual precipitation of the area and its value is 1146.83 mm

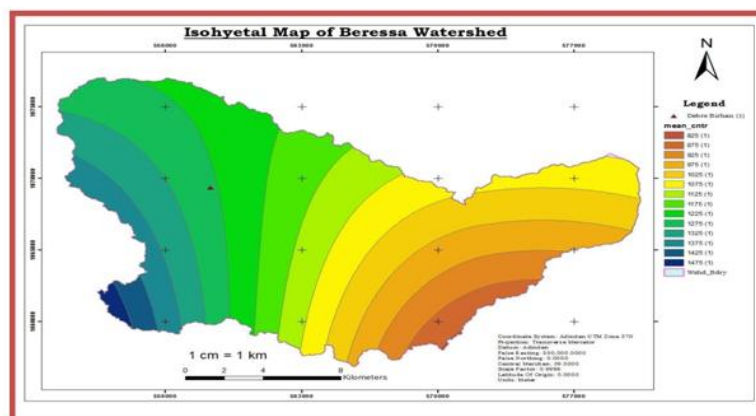


Figure 10: Isohytal map of Beressa Watershed

Month	Jan	Feb	Mar	Apr	May	Jun	Jul	Aug	Sep	Oct	Nov	Dec	Annual
Prec(mm)	10.44	34.53	73.56	88.23	54.17	70.8	252.05	255.96	63.65	22.08	12.71	9.26	947.44

Table 3: Average monthly precipitation of ten years data (2004 - 2013)

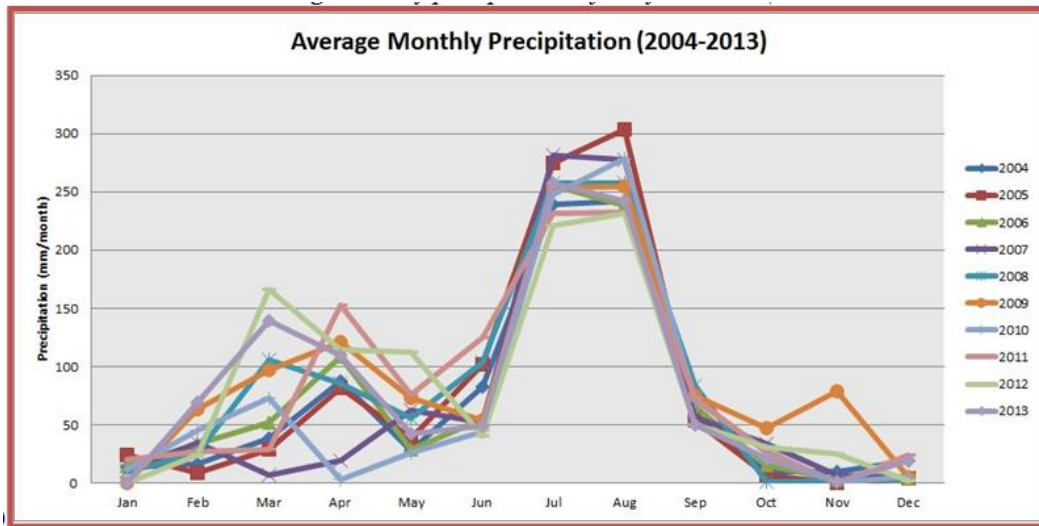


Figure 11: Average monthly precipitation, CFSR data (2004-2013)

b) Evapotranspiration

Evaporation is the process where liquid water is converted to water vapor (vaporization) and removed from sources such as the soil surface, wet vegetation, pavement, water bodies, etc. Transpiration consists of the vaporization of liquid water within a plant and subsequent loss of water as vapor through leaf stomata (Lincoln, Z. et al., 2010).

i. Potential Evapotranspiration

Ten years average air temperature data is taken from Climate Forecast System Reanalysis (CFSR) and potential evapotranspiration is computed using the following formula.

$$Et = 1.6b \left[\frac{10T_a}{I} \right]^a$$

Where, Et. = Potential evapotranspiration incm/month, T_a = Mean monthly air temperature in ($^{\circ}C$), b = latitude correction
 I = annual heat index Using ten year mean monthly air temperature, the annual heat index is calculated as;

$$I = \sum_{i=1}^{12} \left[\frac{T_{a_i}}{5} \right]^{1.5}$$

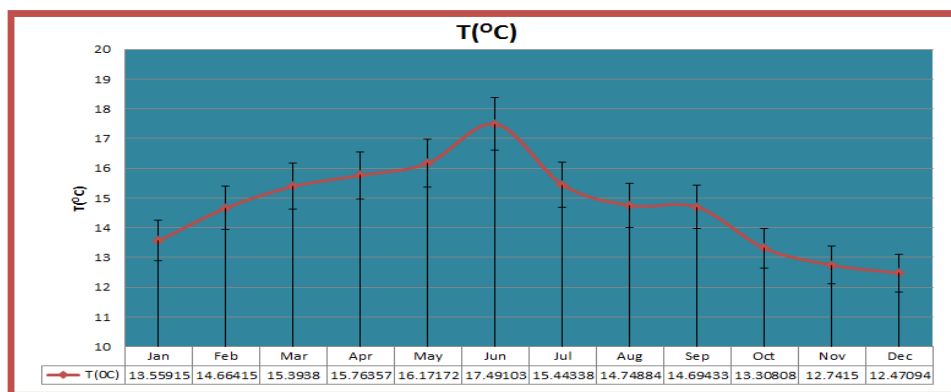


Figure 12: Average Mean monthly air temperature

The mean monthly temperature of the area attains its lowest value in the month of December and increases until June, which is the hottest month in the area. The area has a mean annual temperature of 14.70°C. By substituting the mean monthly air temperature given in the table into the above equation, the value of annual heat index, I , is found to be 60.74 (i.e. $I=60.74$). Then the value of the exponent a can be calculated from the annual heat index using the following formula;

$$a = 0.49 + 0.0179I - 0.0000771I^2 + 0.000000675I^3$$

Then substituting for I , $a = 1.44$

The latitude of the study area is approximated to be $10^{\circ} N$.

Month	Jan	Feb	Mar	Apr	May	Jun	Jul	Aug	Sept	Oct	Nov	Dec
b	0.97	0.98	1.00	1.03	1.05	1.06	1.05	1.04	1.02	0.99	0.97	0.96

Table 4: Latitude correction values of $10^{\circ} N$ Latitude

Using the above parameters, potential evapotranspiration is calculated by substituting these values into the Thornthwaite formula. The values are represented in the graph below.

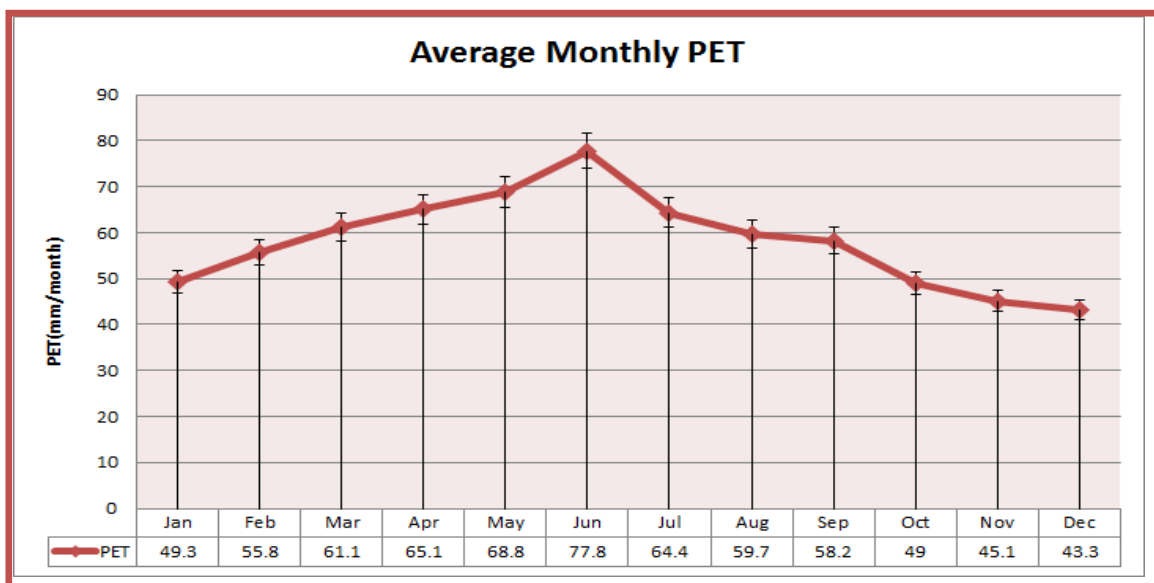


Figure 13: Average monthly Potential evapotranspiration

As we can see from the above graph, the maximum potential evapotranspiration occurs from May to July because in these months the temperature is very high whereas in other months, the potential evapotranspiration is lower since the temperature limits the value of PET.

ii. Actual Evapotranspiration

The most popular method of computing actual evapotranspiration is through the calculation of potential evapotranspiration. Actual evapotranspiration is calculated from potential evapotranspiration with the following procedures (Randall K. Kolka and Ann T. Wolf, 1998):

Step 1: PET- potential evapotranspiration calculated with the Thornthwaite equation. Step 2: P-PET- precipitation less the potential evapotranspiration.

Step 3: Accumulated Potential Water Loss (ACPWL) - accumulated potential water loss, which is the amount of soil water lost when PET exceeds P; i.e., there is less precipitation than potential evapotranspiration. In the calculation of AET, ACPWL is not a factor until P-PET becomes negative. To determine the ACPWL

for a particular month, the previous month's ACPWL and the current month's P-PET are summed. In the original program, ACPWL becomes 0 after a month in which $PET < P$.

Step 4: Soil moisture- soil storage is the maximum soil storage at field capacity (ACPWL = 0). When below field capacity (ACPWL < 0), soil moisture is a function of both maximum soil storage and ACPWL.

Step 5: Delta (change in soil moisture) - the difference between soil storage in successive months when it is less than maximum. When DELTA is negative, then AET < PET

Step 6: Actual Evapotranspiration (AET) - actual evapotranspiration is the sum of available precipitation for the month □ the change in soil moisture. When Delta is positive, AET

$$SM = AWC \exp \left[- \frac{(ACPWL)}{AWC} \right]$$

=PET. When Delta is negative, AET = precipitation for the month + the absolute value of Delta.

Month	Jan	Feb	Mar	Apr	May	Jun	Jul	Aug	Sept	Oct	Nov	Dec	Annual
P	10.44	34.53	73.56	88.23	54.17	70.80	252.05	255.96	63.65	22.08	12.71	9.26	947.44
PET	49.30	55.80	61.10	65.10	68.80	77.80	64.40	59.70	58.20	49.00	45.10	43.30	697.60
P-PET	-38.86	-21.27	12.46	23.13	-14.63	-7.00	187.65	196.26	5.45	-26.92	-32.39	-34.04	
Acc Pot WL	132.21	153.48	141.02	117.89	132.52	139.52				26.92	59.31	93.35	
AWC	200.00	200.00	200.00	200.00	200.00	200.00	200.00	200.00	200.00	200.00	200.00	200.00	
[APWL]	132.21	153.48	141.02	117.89	132.52	139.52	0.00	0.00	0.00	26.92	59.31	93.35	
SM Retained	103.26	92.84	98.81	110.93	103.10	99.56	200.00	200.00	200.00	174.81	148.68	125.41	
ASM	-22.15	-10.42	5.97	12.11	-7.82	-3.55	100.44	0.00	0.00	-25.19	-26.14	-23.27	
AET	32.59	44.95	61.10	65.10	61.99	74.35	64.40	59.70	58.20	47.27	38.85	32.53	641.02

Table 5: Step by step calculation of Actual Evapotranspiration

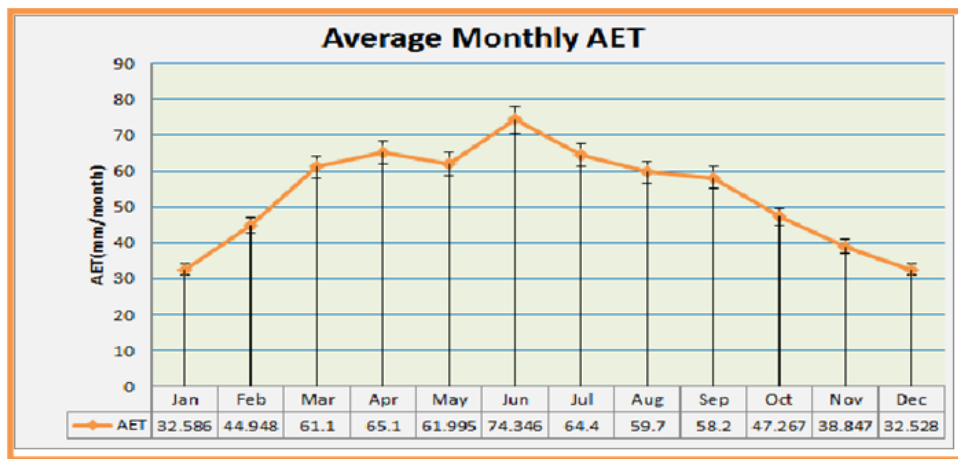


Figure 14: Average monthly actual evapotranspiration

iii. Surface Runoff

Runoff is one of the most important hydrologic variables used in most of the water resources applications. Its occurrence and quantity are dependent on the characteristics of rainfall event, i.e. the intensity, duration and distribution. Apart from these rainfall characteristics, there are a number of catchment specific factors, which have a direct effect on the occurrence and volume of runoff. This includes soil type, vegetation cover; slope and catchment type (Kailas P., 2014). Estimation of direct runoff is done using the curve number method.

Surface runoff is calculated using ten year daily precipitation data which is the sum of the weighted precipitation from four stations obtained from CFSR using the following formula:

$$(P = 0.2S)^2$$

$$Q =$$

$$(P = 0.8S)$$

$$S = \frac{1000}{CN}$$

CN

Where S-is potential maximum retention after runoff begins
 CN-is known as Curve Number as suggested by the American Soil Conservation Service (SCS)
 Q- Volume of runoff in inches P-Rainfall depth in inches

Land use descriptions	A	B	C	D
Commercial, townhouses	80	85	90	95
Cultivated with conventional tillage	72	81	88	91
Forest or woodsthin stand and poor cover	45	66	77	83
Pavement and roofs	100	100	100	100
Pasture or range poor condition	68	79	86	89
Farmsteads	59	74	82	86

Table 6: Some examples of CN values for different types of soils

The Curve Number (CN) value for the study area is approximated to be 86.63 (i.e. CN = 86.63), and using this value potential maximum retention (S) will be;

$$S = (1000/86.63) - 10 = 1.54$$

$$Q = [\sum (P_i - 0.2 \times S) / P + 0.8 \times S] / n = 169.655 \text{ mm}$$

iv. **Groundwater recharge**

Groundwater recharge of the study area is calculated using the water balance method as follows:

$$\text{Groundwater recharge} = \text{Precipitation} - (\text{Actual evapotranspiration} + \text{Surface runoff})$$

By substituting the values of precipitation, Actual evapotranspiration and Surface runoff the value of the groundwater recharge will be:

$$\text{Groundwater recharge (R)} = 947.44 \text{ mm} - 641.017 \text{ mm} - 169.655 \text{ mm} = \underline{\underline{136.768 \text{ mm}}}$$

Generally, as we can see from the chart below from the total precipitation of 947.44 mm, 68% (641.017 mm) of it re-evaporates to the atmosphere, 18% (169.655 mm) follows surface paths as runoff and 14% (136.768 mm) of it percolates through the soil layer to replenish the groundwater.

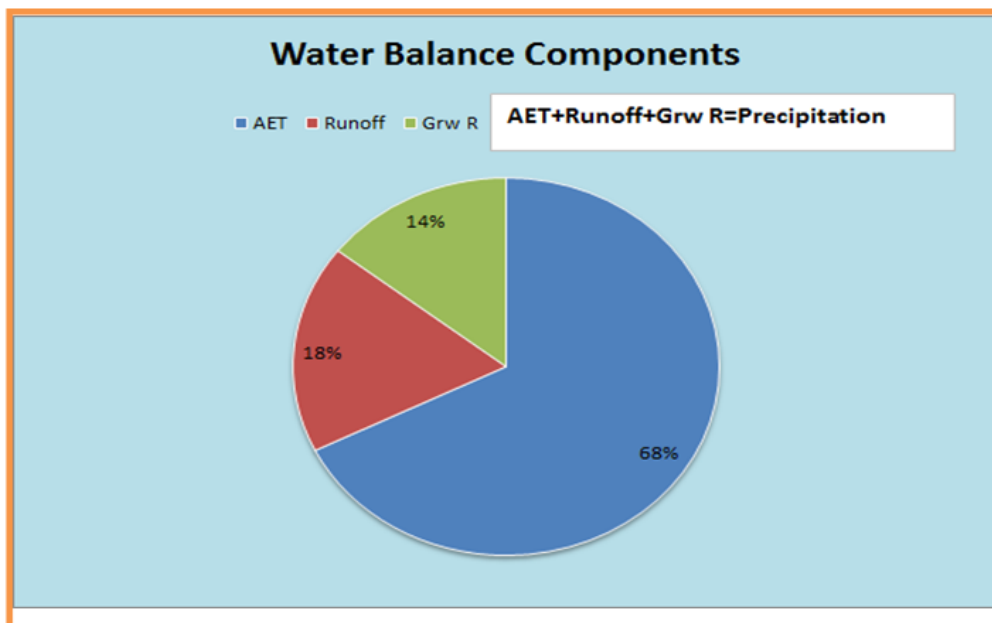


Figure 15: Proportion of the four Water balance components

4.1 **Groundwater Recharge Estimation Using SWAT Model**

The SWAT model is a semi-distributed, time-continuous watershed simulator operating on a daily time step (Arnold et al., 2012). SWAT model takes DEM, LULC, soil data, slope, weather data and stream flow data as an input. The watershed is divided into sub-watershed and the sub-watersheds further into Hydrologic Response Units (HRU). The semi-distributed SWAT model is based on HRUs, which are formed from overlapping maps for soil, LULC and slope. The principle is that each HRU is composed of specific land use; slope and soil classes and they have similar hydrologic characteristics. (Hadilawit Tadesse,

2019). The size of sub-basin in the watershed will affect the assumption of homogeneity. Hence, the definition of a watershed, sub-basin boundaries and streams is decided based on a threshold area to define streams (Megersa et al, 2019). A properly projected DEM of 30 m resolution was loaded to Arc SWAT interface. Then, the DEM was masked and stream networks were recreated using the loaded DEM. The outlet point was selected from the streams, where the two main rivers Beressa and Dalecha Rivers meet. Finally, the sub-watersheds and the boundary of the watershed were delineated based on the outlet point defined before. For defining the HRUs, slope, soil and LULC map were loaded using the Land use/soil/slope definition menu. The soil map and LULC map were reclassified using appropriate look up tables, and the slope map was reclassified in to five classes of different slope value ranges. In SWAT model, PET is calculated using Penman-Monteith, whereas Runoff is estimated with Curve Number method. The results obtained based on 10 year monthly averaged values of the model are represented below.

Hydrologic Parameter	Jan	Feb	Mar	Apr	May	Jun	Jul	Aug	Sep	Oct	Nov	Dec	Annual
PET	127.7	128.5	158.5	153.0	170.7	158.5	104.6	115.7	145.3	138.7	127.4	119.2	1647.8
AET	7.4	17.4	39.2	50.1	60.9	61.2	81.5	94.3	78.3	42.2	23.9	15.9	572.4
Surface Runoff	0.1	0.9	10.4	21.9	7.6	13.1	69.0	86.4	17.1	0.7	1.3	0.0	228.5
Inter Flow	0.5	0.5	0.9	1.3	1.4	1.3	3.6	5.9	4.8	2.8	1.5	0.9	25.5
GW percolation	0.0	0.1	1.9	7.0	1.8	5.0	44.7	55.7	10.0	0.2	0.0	0.0	126.5
Total													952.9

Table 7: Average Hydrologic parameters derived from SWAT model

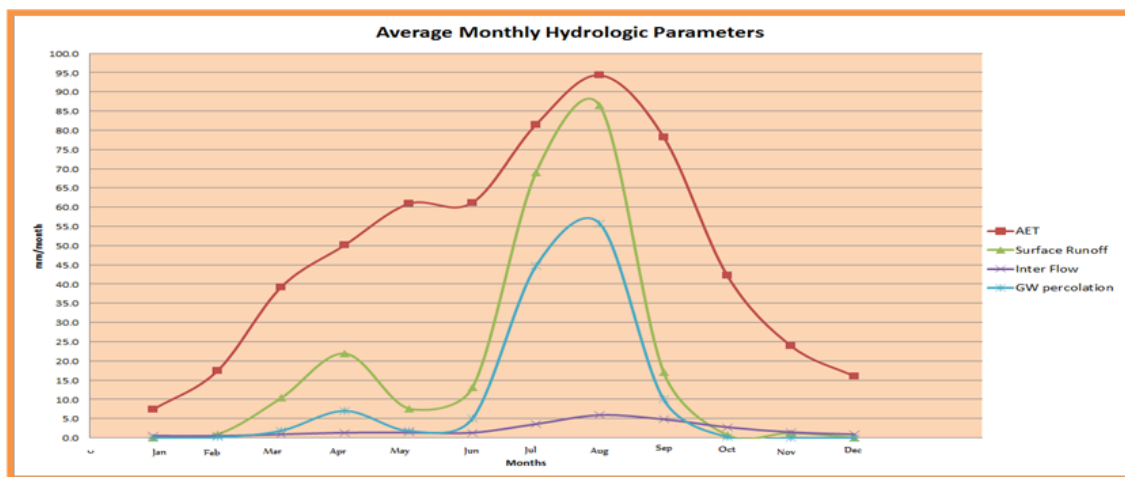


Figure 16: Graph showing average monthly hydrologic parameters calculated using SWAT model

The graph above shows continuous monthly increase in AET from January to August and a decrease until December. August is the month with the highest rate of AET, because it is the month with the highest monthly precipitation and its AET is close to the PET because of increasing soil moisture condition. 254.1mm (44.38 %) of the ET occurs in the wet months (July-September). The GW percolation and Surface runoff shows similar trend, where the three months (July-September) taking the lion's share with 87.34% of Groundwater Percolation and 75.49% of Runoff occurring in these months. There is, however, some appreciable amount of Groundwater percolation and surface Runoff occurring between March and April, because of the presence of short rainy (Belg) season. Interflow shows the least value from the WB components in the watershed. Similarly, it attains its highest values in the wet months, but with a slight deviation to the right, possibly because of the larger time it takes to move through soil particles than surface runoff. The average annual value of these WB components is shown in the figure below along with the paths followed by each component

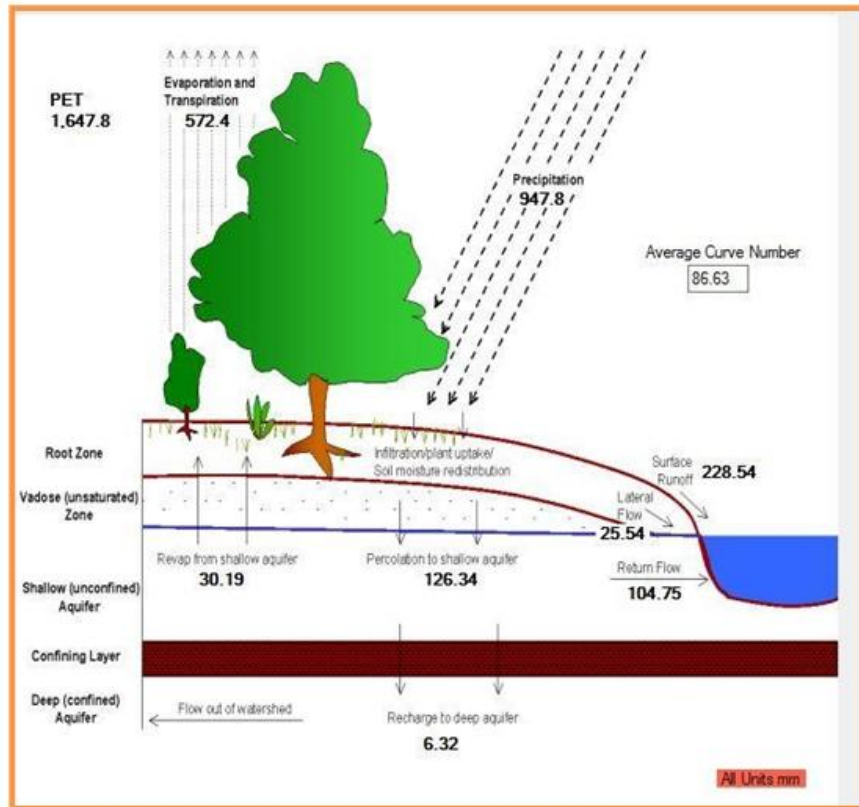


Figure 17: Average annual hydrologic components obtained from SWAT model.

V. DISCUSSION AND SUMMARY

5.1 Comparison of WB and SWAT Models

The annual groundwater recharge estimation of the watershed has been computed using the two methods, and the results have been explained above.

Hydrologic Variables	WB	%fromPrec	SWAT	%fromPrec
Precipitation	947.44		947.44	
PET	697.60		1647.80	
AET	641.02	67.66	572.40	60.42
Surface runoff	169.66	17.91	228.50	24.12
Interflow	0.00	0.00	25.50	2.69
GWrecharge	136.77	14.44	126.50	13.35

Table 8: Comparison of WB and SWAT model for hydrologic variables

The two methods have presented values with some similarity, especially the Groundwater recharge, which is the main concern of this study. Considering the cold climate, and clay-loam soils of the area, the lower AET and higher Surface runoff values of the SWAT model look more reasonable. The SWAT model also presents another aspect of the water balance component, which is sub-soil interflow flow. The annual Groundwater recharge value of the watershed estimated using the two methods, however, is very similar and a mean value of **131.63 mm/year** is adopted for the watershed. This corresponds to **13.89%** of the annual precipitation. This is a very reasonable value considering the high Groundwater potential of the area under study. It is also agreeable to studies conducted in areas around the watershed. Berehanu, B. et al., (2017) have estimated the annual groundwater recharge of Jema sub-basin to be 133mm, 13.39% of the annual precipitation using WB method. Molla Demlie, (2015) estimated the annual groundwater recharge of

Akaki catchment to be 105 mm/a, a catchment with some climatic similarity with Beressa watershed. He referred the above values as the minimum estimate based on data from other methods and field observation. On the other hand, (Tesfaye Chernet, 1988 as cited in Jiri Sima, 2018) classified the different rocks of the area into aquifer groups of moderate yield. General recharge to groundwater from rainfall is estimated to be 50 to 150 mm/year.

5.1 Sustainable Yield

There has been a debate on the applicability of the terms safe yield and sustainable yield among Hydrogeologists. The term safe yield was first used in 1915 to mean the “quantity of water that can be pumped regularly and permanently without dangerous depletion of the storage reserve” (S. J. Meyland, 2011). A misperception among many hydrogeologists and water resources managers is that the development of groundwater is considered to be „Safe“ if the rate of groundwater withdrawal does not exceed the rate of natural recharge. Even with a pumping rate smaller than the natural recharge (so called safe yield), pumping may have induced recharge and decreased discharge. The induced recharge may have caused the depletion of streamflow and residual discharge may not be sufficient to maintain groundwater dependent ecosystems. Furthermore, pumping always creates a cone of depression, which may cause intrusion of bad quality water and land subsidence (Yangxiao Zhou, 2009)

On the other hand, sustainable yield is the extraction and use of groundwater resources in a way that does not create unacceptable environmental, economic, or social consequences (Yangxiao Zhou, 2009). The estimation of sustainable yield of an area requires detail investigation and modeling of the aquifer system and interaction with the ecosystem of the area. However, (S. J. Meyland, 2011) indicate that a set aside of anywhere from 10 to 40% of annual GW recharge seems reasonable.

Taking the highest value of the above assumption, it is assumed that 40% of the annual GW recharge (52.65 mm) can be extracted annually without adversely affecting the natural ecosystem of the area. In volumetric terms, 44.83 MCM is being recharged annually for the total watershed, from which **17.93 MCM** is the sustainable yield.

6. Conflicts of Interest

We declare that there is no conflict of interest regarding the publication of this paper.

References

- [1]. Arnold, J. G., Moriasi, D. N., Gassman, P. W., Abbaspour, K. C., White, M.J., Srinivasan, R., Santhi, C., (2012). SWAT: Model Use, Calibration, and Validation”, *Transactions of the ASABE*, 55/4: 1491–508.
- [2]. Belete Berhanu, Assefa M. Melesse and Yilma Seleshi (2013). GIS-based hydrological zones and soil geo-database of Ethiopia, *Catena* 104, 21–31
- [3]. Berehanu, B., Azagegn, T., Ayenew, T. and Masetti, M. (2017). Inter-Basin Groundwater Transfer and Multiple Approach Recharge Estimation of the Upper Awash Aquifer System. *Journal of Geoscience and Environment Protection*, 5, 76-98.
- [4]. Ciach GJ. (2003). Local random errors in tipping-bucket rain gauge measurements. *Journal of Atmospheric and Oceanic Technology*, 20 (5): 752-759.
- [5]. Cook P. G., Walker, G. R. and Jolly, I. D., (1989). Spatial Variability of Groundwater Recharge in a Semi-Arid Region. *Journal of Hydrology*, 111: 195-212.
- [6]. Daniel Meshesha, Dejene Haile Mariam and Abrham Mammo, (2000). Geology of Debre Birhan Area, unpublished report. Geological Survey of Ethiopia (GSE)
- [7]. Daniel R. Fuka, M. Todd W., Charlotte M., Arthur T., Tammo S., Steenhuis and Zachary M. (2013). Using the Climate Forecast System Reanalysis as Weather Input Data for Watershed Models. *Hydrology Process*. Wiley Online Library (wileyonlinelibrary.com).
- [8]. Department of Agricultural & Plantation Engineering, Open University, Nawala, Nugegoda 10250, Sri Lanka (2004). Spatial Variability of Groundwater Recharge. *Journal of Spatial Hydrology*, 4(1), 1-18.
- [9]. FAO/IIASA/ISRIC/ISS-CAS/JRC (2009). Harmonized World Soil Database (version 1.1), FAO, Rome, Italy and IIASA, Luxembourg, Austria
- [10]. Hadilawit Tadesse (2019). Effects of Land Cover Change on Water Balance Component in Gilgel Abay Catchment Using SWAT Model. Unpublished MSc Thesis, Faculty of Geo-Information Science and Earth Observation, University of Twente.
- [11]. Horton, R. E., (1932). Drainage-Basin Characteristics, *Eos Trans. AGU*, 13, 350-361. http://geoportal.rcmrd.org/layers/servir%3Aethiopia_sentinel2_lulc2016http://opentopo.sdsc.edu/datasetshttp://www.fao.org/geonetwork/srv/en/metadata.show?id=14116
- [12]. Jiri Sima (2018). Hydrogeological and hydrochemical maps of Debre Birhan (NC 37-11) mapsheet, Czech Geological Survey, Prague; Geological Survey of Ethiopia, Addis Ababa. Unpublished report.
- [13]. Kailas P., (2014). Estimation of Runoff by using SCS Curve Number Method and Arc GIS. *International Journal of Scientific & Engineering Research*, 5, 1283-1287.
- [14]. Ketema Tilahun & Broder J. Merkel (2009). Estimation of groundwater recharge using a GIS-based distributed water balance model in Dire Dawa, Ethiopia, *Hydrogeology Journal*, 17: 1443–1457.
- [15]. Kevin M. Hiscock. (2005). *Hydrogeology: Principles and Practice*. Blackwell Publishing, Oxford, UK.
- [16]. 16. Kouwen N, Danard M, Bingeman A, Luo W, Selenieks, FR, Soulis, ED. (2005). Case study: watershed modeling with distributed weather model data. *Journal of Hydrologic Engineering*, 10(1): 23-38.
- [17]. Lincoln, Z., Michael, D., Consuelo, C., Kati, W., and Kelly, T. (2010). Step by Step Calculation of the Penman-Monteith Evapotranspiration (FAO-56 Method). IFAS Extension Service, University of Florida, 1-10.
- [18]. Meha VK, Walter MT, Brooks ES, Steenhuis TS, Walter MF, Johnson M, Boll J, Thongs D (2004). Evaluation and application of

- SMR for watershed modelling in the Catskill Mountains of New York State. *Environmental Modelling and Assessment*. **9** (2): 77-89.
- [19]. MollaDemlie (2015). Assessment and estimation of groundwater recharge for a catchment located in highland tropical climate in central Ethiopia using catchment soil–water balance (SWB) and chloridemass balance (CMB) techniques, *Environ Earth Sci*.
- [20]. NMSA. (2001). Initial National Communication of Ethiopia to the United Nations Framework Convention on Climate Change (UNFCCC), Federal Democratic Republic of Ethiopia, Ministry of Water Resources, National Meteorological Services Agency
- [21]. R. Allan Freeze and John A. Cherry (1979). *Groundwater*, Prentice-Hall, Inc, New Jersey
- [22]. Randall K. Kolka and Ann T. Wolf (1998). Estimating Actual Evapotranspiration for Forested Sites: Modifications to the Thornthwaite Model. United States Department of Agriculture, 2pp.
- [23]. S. J. Meyland (2011). Examining safe yield and sustainable yield for groundwater supplies and moving to managed yields as water resource limits become a reality, *Water Resources Management* **18**:1-3
- [24]. Saeid Eslamian. (2014). *Handbook of Engineering Hydrology: Fundamentals and Applications*. Taylor & Francis Group, New York
- [25]. Teklebirhan, A., Dessie, N. and Tesfamichael, G. (2012). Groundwater Recharge, Evapotranspiration and Surface Runoff Estimation Using WetSpa Modeling Method in Illala Catchment, Northern Ethiopia. **4**(2):96-110.
- [26]. Tim Davie (2008). *Fundamentals of Hydrology*. Second edition, Taylor & Francis Group, New York
- [27]. Tolera, M., Dessie N., and Mekuria A. (2019). Combined effect of land use/cover types and slope gradient in sediment and nutrient losses in Chancho and Sarga sub watersheds, East Wollega Zone, Oromia, Ethiopia. *Environmental Systems Research*. Springer Online publisher, 1-14.
- [28]. WMO (1985). Review of requirements for area-average precipitation data, surface-based and space-based estimation techniques, space and time sampling, accuracy and error; data exchange. WCP-100, WMO/TD-No. 115, 57pp.
- [29]. Yangxiao Zhou (2009). A critical review of groundwater budget myth, safe yield and sustainability, *Journal of Hydrology*, **370**: 207-213.
- [30]. Zewdu Alebachew (2011). Analysis of Urban Growth and Sprawl Mapping Using Remote Sensing and Geographic Information System (Case Study of Debre Birhan Town), Unpublished MSc Thesis, Addis Ababa University.